

# Doppler-Broadening of Annihilation Radiation Spectroscopy under High Magnetic Field Using a Longitudinally Spin-polarized Slow Positron Beam

Masaki Maekawa, Hongjun Zhang, Hui Li, Yuki Fukaya, and Atsuo Kawasuso

Japan Atomic Energy Agency, Takasaki, Gunma 370–1292, Japan

E-mail: maekawa.masaki@jaea.go.jp

(Received Jun. 11, 2014)

A spin-polarized positron beam generated using a  $^{22}\text{Na}$  source, solid neon moderator and magnetic lens was developed. The beam diameter, beam flux and spin polarization were 0.5 mm,  $1 \times 10^5 \text{ e}^+ \text{ s}^{-1}$  and 27 %, respectively. An electromagnet system, which can generate  $\pm 1$  T magnetic field, was also developed and equipped with the beam apparatus. Using this apparatus, Doppler broadening of annihilation radiation spectra under a high magnetic field were measured for bulk polycrystalline Fe, Co and Ni samples and a thin film  $\text{Co}_2\text{MnSi}$  sample. These spectra showed a clear asymmetry upon field reversal.

## 1. Introduction

For further research of spintronics materials, the evaluation of electron spin is an important issue. A new technique, “spin-polarized positron annihilation spectroscopy” (SP-PAS) method, is one of such advanced methods to evaluate electron spin polarization at the surface, interface and in the bulk. The pair-annihilation probability of a positron and an electron depends on their relative spin direction. Hence, when both positrons and electrons are spin-polarized, the positron-electron momentum distribution shows an asymmetry upon spin reversal. We have demonstrated that the Doppler broadening of annihilation radiation (DBAR) technique with spin-polarized positrons can be used for studying ferromagnetic band structures [1, 2]. Since novel spin-phenomena occur at surfaces and/or interfaces and in thin films, a variable-energy spin-polarized slow positron beam needs to be developed.

In recent years, we have developed spin-polarized beams with  $^{68}\text{Ge}$  and  $^{22}\text{Na}$  sources [3, 4]. The longitudinal spin polarization of the slow positron beam generated using a  $^{68}\text{Ge}$  source (47 %) is higher than that using a  $^{22}\text{Na}$  source (25 %–30 %) [5]. The half-lives of  $^{68}\text{Ge}$  and  $^{22}\text{Na}$  are 280 days and 2.6 years, respectively. These sources are suited for a SP-PAS experiment. We showed that a high brightness positron beam can be produced using a solid neon moderator without losing longitudinal spin polarization [6, 7].

Employing a longitudinally spin-polarized positron beam, longitudinal excess electron spins in magnetic substances under a strong magnetic field can be estimated. For such measurements, the maximum field strength of the magnetic field is important. Although there are some reports about construction of a magnet system for the *in situ* PAS measurements using a slow positron beam [8, 9], in most cases the maximum field strength was limited. Generally, it is difficult to introduce a light-weight charged-particle beam, such as slow positron beam, into a strong magnetic field because such a light particle is easily deflected when it crosses magnetic flux lines. In other words, a slow positron beam implanted to the magnetic field completely horizontally can penetrate the strong magnetic field and reach the sample. For this, it is important to reduce the beam divergence and leakage magnetic field from the electrostatic magnet. In this study, to carry out *in situ* DBAR measurement in high magnetic field we constructed an electromagnet system which is connected to the high brightness

positron beam.

## 2. Beam development

Figure 1 shows an overview of the newly developed beam apparatus. A 330 MBq  $^{22}\text{Na}$  source was deposited into a 2-mm-diameter hole and sealed by a 5- $\mu\text{m}$ -thick Ti cap. The source was cooled down to 4 K and a solid neon film was grown on the source window as a moderator [6]. A slow positron beam with energy of 15 keV was generated by a modified Soa-gun [10]. The positron beam was transported by four magnetic lenses and focused onto the sample located inside an electromagnet.

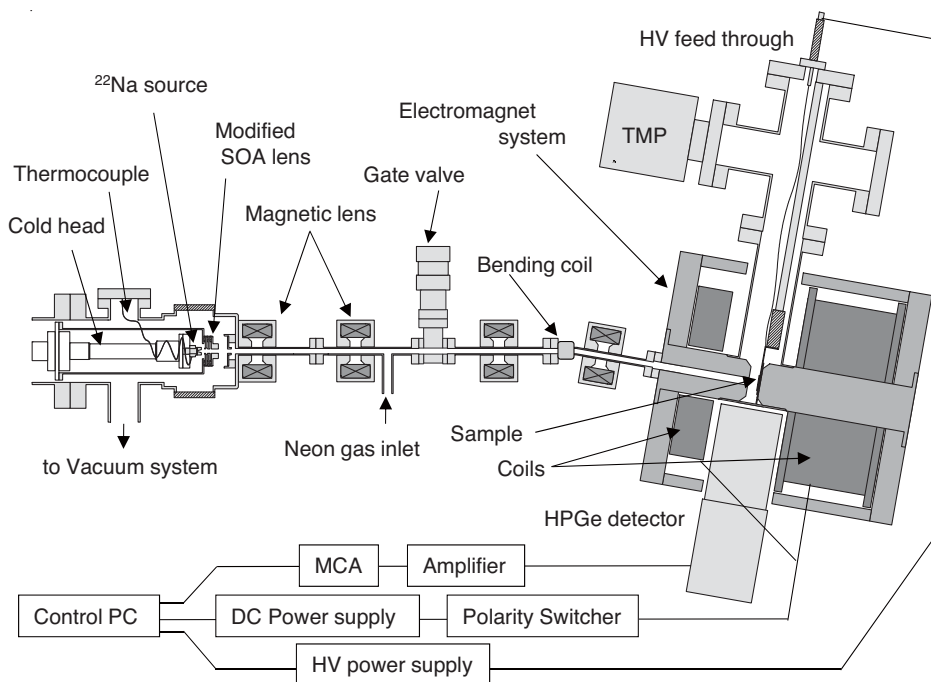


**Fig. 1.** Schematic of the spin-polarized positron beam apparatus equipped with an electromagnet system. A high brightness positron beam generated by a small source and a solid Ne moderator is introduced into the magnetic field for the *in situ* DBAR measurement.

Figure 2(a) shows a schematic of the electromagnet system. The sample is placed in the gap between the two pole pieces and the slow positron beam is injected into the magnetic field through the entrance hole. The pole pieces are made from electromagnetic soft iron with a diameter of 60 mm. Two normal conducting coils are used to generate the magnetic field. Figure 2(b) shows the result of a numerical calculation of the magnetic field around the sample. When the pole pieces are magnetically saturated, the magnetic field at the sample position reaches 1 T.

Magnetic flux lines near the pole piece obtained from the calculation are also illustrated in Fig. 3(a). At the exit of the beam hole of the pole piece and the sample position, positrons feel the magnetic field  $B = B_0$  and  $B = B_1$ , respectively (see Fig. 3(b)). When the magnetic field is changed gradually, the magnetic moment of the positron is preserved. Here,  $V$  is positron velocity,  $v_r$  and  $v_z$  are its vertical and parallel components to the beam axis and  $\theta$  is the initial beam divergence angle,

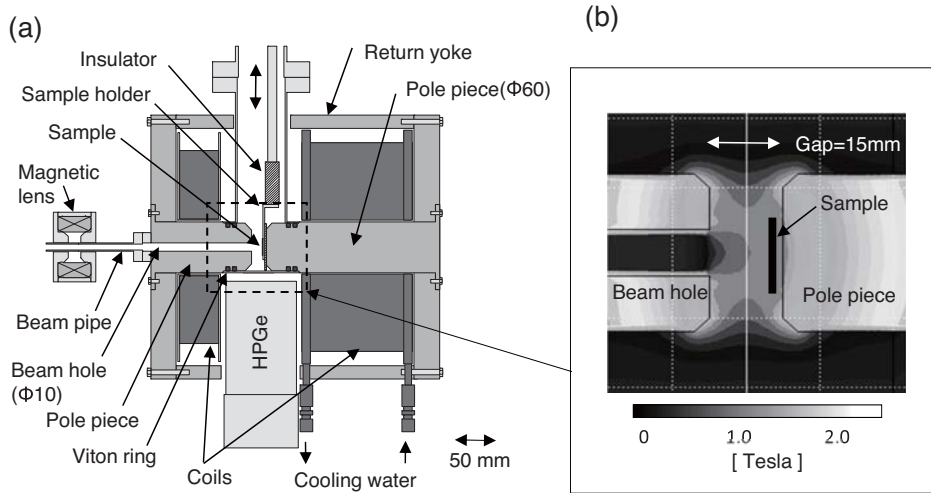


**Fig. 2.** (a) Details of the electromagnet. (b) Result of the numerical calculation of the magnetic field strength near the pole piece is also shown.

the vertical velocity components are described by the mirror effect as follows.

$$\frac{\frac{1}{2}mv_{0r}^2}{B_0} = \frac{\frac{1}{2}mv_{1r}^2}{B_1} \quad (1)$$

Using  $V^2 = v_{0r}^2 + v_{0z}^2 = v_{1r}^2 + v_{1z}^2$ ,  $v_{0z} = V \cos \theta$  and  $v_{0r} = V \sin \theta$ , we obtain the parallel velocity component at sample position.

$$v_{1z}^2 = V^2 \left( 1 - \frac{B_1}{B_0} \sin^2 \theta \right) \quad (2)$$

When  $v_{1z} < 0$ , positrons will be repelled by the magnetic mirror effect and cannot reach the sample. We finally obtain the simple equation which determines the maximum initial beam angle at which positrons can penetrate the mirror field or not.

$$\sin \theta = \sqrt{\frac{B_0}{B_1}} \quad (3)$$

The distance between the sample and the final magnetic lens is 220 mm and the inner diameter of the beam pipe is 7 mm. If the beam diameter at the sample position is assumed to be 0.5 mm,

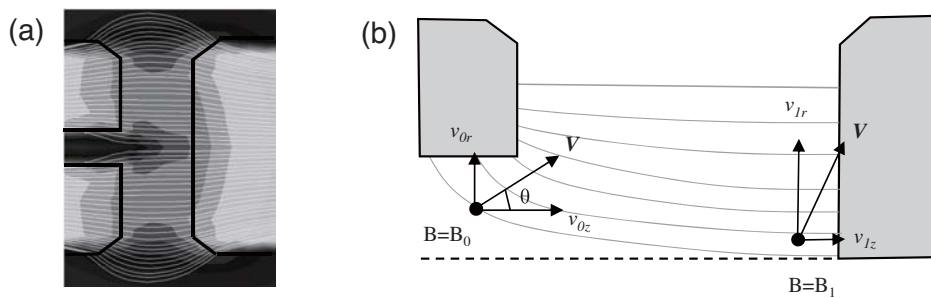


**Fig. 3.** (a) Magnetic flux lines near the pole piece obtained from a calculation. (b) Illustration of the velocity components near the sample position.

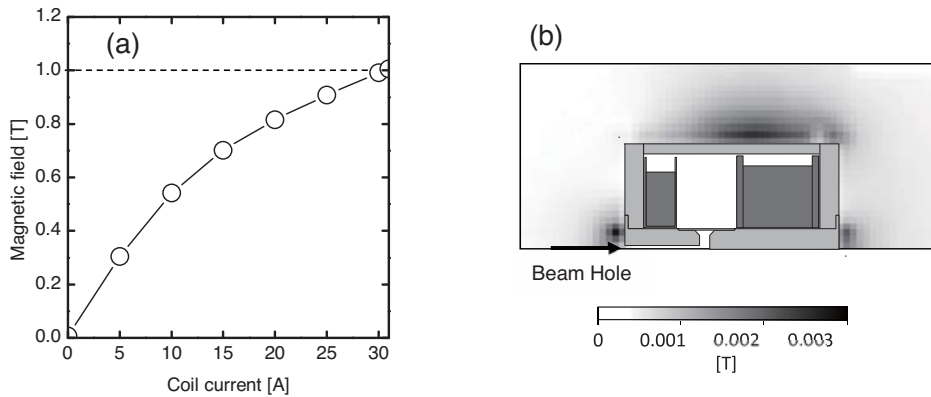


**Fig. 4.** (a) The magnetic field strength at the sample position measured as a function of coil current. (b) Calculated magnetic field leakage around the electromagnet yoke.

maximum beam divergence angle obtained from the geometry is estimated to be  $\theta = \arctan((3.5 + 0.25)/220) = 0.98^\circ$ . When the beam energy is 15 keV,  $v_{0r}$  and  $v_{0z}$  are the velocity corresponding 0.23 eV and 14.99 keV, respectively. Using the magnetic field strengths of  $B_1 = 1$  T and  $B_0 = 0.01$  T, which are picked up from the result of the numerical calculation,  $v_{1z}$  is estimated to be 14.56 keV. In this condition, if the positron incident energy deviates by more than 0.44 keV from 15 keV the positron may be lost, however, this component is expected to be small. It was confirmed that the positron beam can reach the sample without significant loss.

It is also important to reduce the magnetic field leakage from the electromagnet. This may cause a deflection of the positron beam and an increase of  $v_{1r}$  and  $\theta$ . We attempted to reduce such field leakage by an iron cover (return yoke) surrounding the coils. Reduction of the leakage magnetic field and the rotational-symmetry of the pole piece prevent the slow positron beam from deflection in one specific direction.

Figure 4(a) shows the measured magnetic field strength at the sample position for the various coil current of the developed magnet. The maximum field strength was confirmed to be 1 T. This result is good agreement with the numerical calculation shown in Fig. 2. Figure 4(b) also shows the leakage of the magnetic field and suggests no significant leakage field on the beam axis that may affect beam transportation.

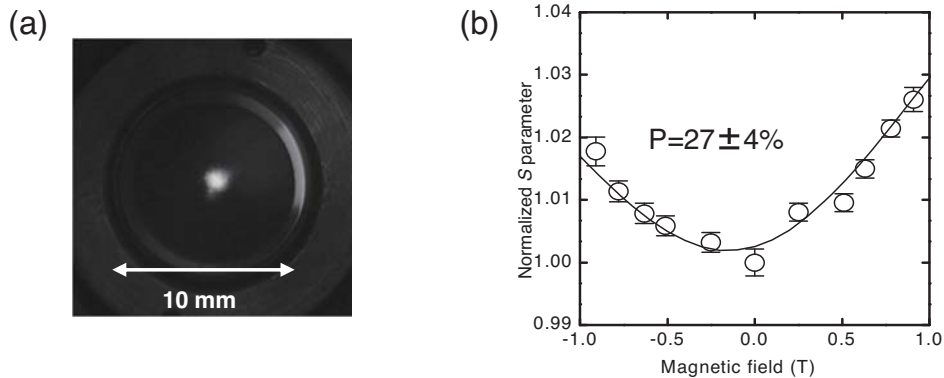


**Fig. 5.** (a) Typical beam image at the sample position, (b) the magnetic field dependence of the  $S$  parameter in fused silica. The spin polarization is estimated to be 27 %.

Before DBAR measurements, the positron beam was observed by a microchannel plate at the sample position. A typical beam image is shown in Fig. 5(a). The beam diameter was 0.5 mm. The beam intensity measured by the HPGe detector was  $1 \times 10^5 \text{ e}^+ \text{ s}^{-1}$  a considerable improvement from the previous  $^{68}\text{Ge}$ -based apparatus [4]. Changing the magnetic field from 0 to  $\pm 1 \text{ T}$ , the beam diameter, position and intensity did not change significantly. This shows that positron beam was injected to the sample without loss.

The longitudinal spin polarization of the positron beam was measured from the magnetic quenching of the positronium in fused silica, which is a simpler method than measuring the positronium decay rate [4, 11–13]. The magnetic field dependence of the  $S$  parameter [4] in fused silica and the estimated spin polarization is shown in Fig. 5(b). A spin polarization of  $27 \pm 4 \%$  is obtained, which is smaller than the  $^{68}\text{Ge}$ -based beam (47 %)[4]. However, the SP-PAS measurement is possible because of an improved counting rate due to the high beam intensity.

### 3. DBAR measurements on ferromagnetic materials

Two types of samples were used for the *in situ* DBAR measurement in the high magnetic field. The first type was ferromagnetic bulk samples with a size of  $10 \text{ mm} \times 10 \text{ mm}$  and thickness of 1 mm. For this measurement, pure Fe (99.99 %), Co (99.9 %) and Ni (99+ %) were used. After mechanical and electrochemical polishing, the samples were heated at  $1200 \text{ }^\circ\text{C}$  for 24 hours in vacuum. Prior to installation onto a sample holder, these samples were polished electrochemically again. The other sample was a chemical-vapor-deposition-grown  $\text{Co}_2\text{MnSi}$  (CMS) film on a MgO substrate. CMS is a half-metal material and is expected to show large deviations for the alternate magnetic field because half-metal materials have completely different band structure for major and minority spins. The thickness of the CMS film was 500 nm. When the incident energy of the positron beam is set to 5 keV, all the positrons will be implanted only in this film.

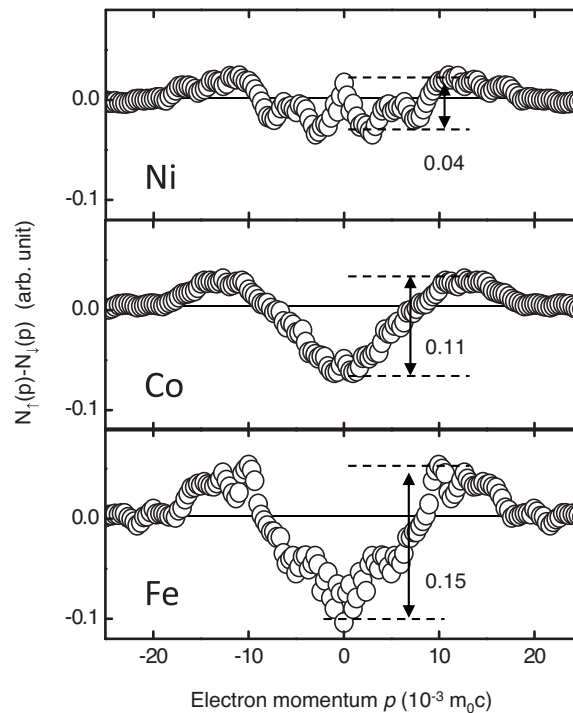


**Fig. 6.** The differential DBAR spectra of bulk ferromagnetic samples in a magnetic field of  $\pm 0.96 \text{ T}$ .

Figure 6 shows the differential DBAR spectra of bulk ferromagnetic samples in a magnetic field of  $\pm 0.96$  T when the positron beam energy was set to 15 keV. This differential spectrum  $[N_{\uparrow(\rho)} - N_{\downarrow(\rho)}]$  was obtained by altering the field polarity. The subscript  $\uparrow$  or  $\downarrow$  indicates whether the positron polarization and the magnetic field direction was parallel or anti-parallel. The total spectrum area contained more than  $1 \times 10^6$  events and the intensities were normalized to unity. A finite differential intensity means that there is a field-reversal asymmetry, which arises from the enhanced annihilation between the spin-up positrons and spin-down 3d unpaired electrons [14, 15]. The differential amplitude of Fe, Co and Ni is 0.04, 0.11 and 0.15, respectively. It was reported that the differential amplitude is proportional to the effective magnetization [1]. In this study, the same tendency is observed. This result also shows that our positron beam was sufficiently spin-polarized.

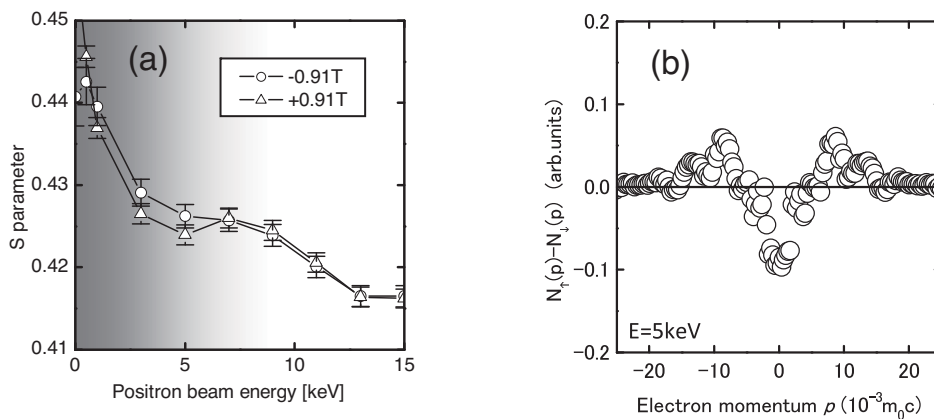


**Fig. 7.** (a) The  $S-E$  curve obtained from the measurement of CMS film sample. The shaded area corresponds to the CMS layer. (b) The differential DBAR spectrum at  $E = 5$  keV.

Figure 7(a) shows the  $S-E$  curve obtained from the measurement of the CMS film sample. By alternating the magnetic field direction, the  $S$  parameter shows an asymmetry in the CMS layer ( $E < 5$  keV), though the  $S$  parameter in the substrate MgO region ( $E > 8$  keV) was not changed. Figure 7(b) shows the differential DBAR spectrum at  $E = 5$  keV. This is due to the effect of d-electrons in the CMS layer. SP-PAS measurement with a spin-polarized slow positron beam is able to determine the depth profile of the excess spins from the surface to the bulk region.

#### 4. Summary

A spin-polarized positron beam generated using a  $^{22}\text{Na}$  source, a solid neon moderator and magnetic lenses was developed. A spin polarization of 27 % was estimated, which is high enough for the SP-PAS measurement. This parallel beam was suitable for injection to the sample in the strong magnetic field generated by an electromagnet system because reflection by the mirror-effect could be suppressed. Using this system, *in situ* DBAR measurements under a strong magnetic field were carried out for polycrystalline Fe, Co and Ni bulk and CMS thin film samples. These spectra showed clear asymmetry upon field reversal.

#### References

- [1] A. Kawasuso, M. Maekawa, Y. Fukaya, A. Yabuuchi, and I. Mochizuki, Phys. Rev. B **83** (2011) 100406(R).
- [2] A. Kawasuso, M. Maekawa, Y. Fukaya, A. Yabuuchi, and I. Mochizuki: Phys. Rev. B **85** (2011) 024417.

- [3] M. Maekawa, Y. Fukaya, Y. Yabuuchi, and A. Kawasuso: J. Phys. Conf. Ser. **262** (2011) 012035.
- [4] M. Maekawa, Y. Fukaya, A. Yabuuchi, I. Mochizuki, and A. Kawasuso: Nucl. Instrum. Methods Phys. Res. Sect. B-Beam Interact. Mater. Atoms **308** (2013) 9.
- [5] A. Kawasuso and M. Maekawa: Appl. Surf. Sci. **255** (2008) 108.
- [6] M. Maekawa, A. Kawasuso, T. Hirade, and Y. Miwa: Mater. Sci. Forum **607** (2009) 266.
- [7] M. Maekawa, Y. Fukaya, H. Zhang, H. Li, and A. Kawasuso: J. Phys.-Conf. Ser. **505** (2014) 012033.
- [8] P. W. Zitzewitz, J. C. Van House, A. Rich, and D. W. Gidley: Phys. Rev. Lett. **43**(1979) 1281.
- [9] T. Kumita, *et al.*: Appl. Surf. Sci. **116** (1997) 1.
- [10] F. J. Mulligan and M. S. Lubell: Meas. Sci. Technol. **4** (1993) 197.
- [11] Y. Nagashima and T. Hyodo: Phys. Rev. B **41** (1990) 3937.
- [12] Y. Nagai, Y. Nagashima, J. Kim, Y. Itoh, and T. Hyodo: Nucl. Instrum. Methods Phys. Res. Sect. B-Beam Interact. Mater. Atoms **171** (2000) 199.
- [13] T. Hirade: Mater. Sci. Forum **445–446** (2004) 234.
- [14] T. W. Mihalisin and R. D. Parks, Phys. Lett. **21** (1966) 610.
- [15] P. Genoud, A. K. Singh, A. A. Manuel, T. Jarlborg, E. Walker, M. Peter, and M. Weller: J. Phys. F **18** (1988) 1933.